LU TP 15-23
June 2015

Light-like Wilson lines at next-to-next-to-leading order

Viktor Svensson

Department of Astronomy and Theoretical Physics, Lund University

Master thesis supervised by Alexey Vladimirov and Roman Pasechnik

Abstract

In this thesis, we consider basic properties of Wilson lines, with special attention devoted to the renormalization and exponentiation property. We describe the generating function approach to non-abelian exponentiation and perform the calculation of the correlator of two and three semi-infinite Wilson lines meeting at a single point to two-loop order. We consider Wilson lines on lightcone and regularize infrared divergences with a δ-regulator. The three line calculation is done within the generating function approach. Using this calculation, we derive the cusp anomalous dimension and soft anomalous dimension at two-loop order. We discuss the problems arising from the use of the δ-regulator for lightlike Wilson lines, and conclude that this regularization is inappropriate for higher-loop calculation. The obtained result is to be used for higher order analysis of the soft factor and can be used for application in multi-hadron factorization theorems, threshold resummation, etc.

Contents

1 Introduction

Wilson lines are non-local operators in quantum field theory that may be thought of as a string of the gauge field [1]. They play an important role in describing the long distance behaviour of forces and can be used to reformulate quantum field theory in terms of loops. In this thesis, we consider properties of Wilson lines within perturbation theory.

Wilson lines and loops can be applied in the description of hadronic processes in quantum chromodynamics (QCD). In QCD, many processes factorize into a soft and a hard part, or a long-distance and a short-distance part [2] [3]. The hard part can be treated within perturbation theory. The soft part involves non-perturbative effects and is usually parametrized by phenomenological functions (parton distributions). Wilson lines are an important ingredient in factorization theorems, since they help to reconstruct the infrared divergences of hadronic processes [4]. In any gauge theory, Wilson lines encode the effect of soft radiation, i.e. the emission of low energy gauge bosons. The detailed description of how soft emissions of a highly energetic particle is described by a Wilson line along the path of the particle can be found in introductory textbooks on QFT such as [2, 5, 6].

In this paragraph, we write down the definition of a Wilson line and introduce necessary notation. A Wilson line between points a and b along the path C looks like

$$\Phi(a,b;C) = \mathcal{P}\exp\left(-ig\int_a^b dz^\mu A_\mu(z)\right) \tag{1.1}$$

$$= 1 - ig\int_a^b dz^\mu A_\mu(z) - g^2\int_a^b dz_1^{\mu_1}\int_{z_1}^b dz_2^{\mu_2} A_{\mu_1}(z_1)A_{\mu_2}(z_2) + \dots \tag{1.2}$$

where the symbol $\mathcal{P}$ denotes path-ordering, A_μ is the gauge field and g is the coupling constant. The gauge field A_μ is a matrix valued field, it can be written in terms of a basis of matrices t^a, called generators, as $A_\mu^a t^a$. The generators t^a can belong to any representation of the gauge group. In general, generators do not commute, so the order is important. Path-ordering specifies that the fields further along the path should be written to the right of earlier fields. The function $\mathcal{P}\exp$ should be interpreted as the application of $\mathcal{P}$ to the power series of the exponential.

Wilson lines possess important properties under gauge transformations. The corresponding transformation for the gauge field has the form

$$A_\mu(z) \to U(z)A_\mu(z)U^\dagger(z) - \frac{i}{g}(\partial_\mu U(z))U^\dagger(z),$$

where $U(z)$ is a matrix of the gauge group. It implies that the Wilson line transforms as

$$\Phi(a,b) \to U(a)\Phi(a,b)U^\dagger(b),$$

which we prove in section 3. In particular, it implies that Wilson loops (lines where the endpoints coincide) are gauge invariant. Partly because of this, a reformulation of gauge theories in terms of loops rather than the gauge field has been investigated [7, 1, 8, 9].

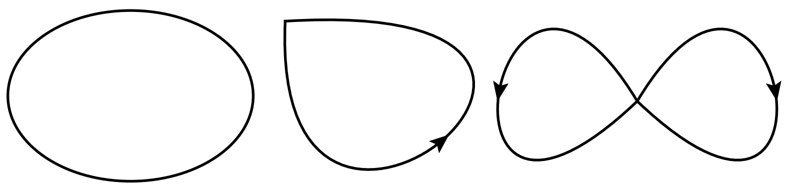

Figure 1: Some important classes of loops. A smooth, a cusped, and a cusped crossed loop.

Nowadays, Wilson lines are used in nearly all branches of quantum field theory (QFT), from the study of confinement [10] to lattice calculations.

One of the most involved problems in perturbative descriptions of Wilson lines is the consideration of their renormalization properties. The main difficulty is that Wilson lines do not have a natural scale. This means that infrared singularities mix with ultraviolet singularities. On the other hand, ultraviolet singularities can be described with the renormalization group equation, which give us hope to resolve the infrared singularities as well [11].

It is known that smooth Wilson loops (left diagram in figure 1) are ultraviolet finite in the renormalized theory [1, 12]. However, the cusped Wilson line or self-intersecting Wilson lines (center and right diagram of figure 1, correspondingly) needs additional renormalization constants [13]. The renormalization constants are governed by the cusp anomalous dimension. The cusp anomalous dimension has been known to two loop-order for a long time [14]. Recently, the three-loop cusp anomalous dimension was found [15].

Wilson lines on lightcone are of special interest. Such Wilson lines appear in the description of hard processes where one can neglect the mass of partons, which is the most typical case. The lightlike Wilson lines have additional infrared divergences [14]. Although this problem has been known for 30 years, there is no clear description of renormalization in this situation. This thesis is devoted to the derivation of the anomalous dimension of several lightlike Wilson lines meeting at a point.

In this thesis, we consider the basic properties of Wilson lines. Our main interest is devoted to the renormalization of Wilson lines, especially to the case of several lightlike Wilson lines meeting at a single point. Such a configuration is called soft anomalous dimension matrix, and is of great importance in the phenomenology of high energy processes with many jets (for recent reviews, see [16, 17]).

We describe a generating function approach to non-abelian exponentiation, which was recently presented in [18, 19]. With the help of that method, we perform detailed two-loop analysis of the soft anomalous dimension for lightlike Wilson loops. As regulator for soft divergences, we use a modified δ-regularization. For regulation of ultraviolet (UV) divergences, we use dimensional regularization. The two-loop calculation of this particular combination of regulators is novel. We have shown that the δ-regulator has a number of problems arising at two-loops, such as violation of gauge invariance and scale invariance. These problems are not observed in the one-loop calculations. We present solutions to these problems. Although we observe artificial terms in the two-loop cusp anomalous dimension. The dipole factorization of the soft anomalous dimension at two-loops is confirmed [20, 21].

The structure of the thesis is the following. In the first section, we review necessary elements of non-abelian gauge theories and perturbative expansion. In section 3, we present derivations of important properties of Wilson lines and following that, we introduce the generating function approach for Wilson lines [18, 19]. Sections 4 and 5 are the main parts of the thesis where we present our approach to lightlike Wilson lines and give details on the two-loop calculation of the soft anomalous dimension. The collection of equations needed is given in the appendices.

2 Elements of QFT and non-abelian gauge theories

2.1 Renormalization

This section contains a brief introduction to renormalization and dimensional regularization, more details can be found in any textbook on QFT such as [5, 6]. Two kinds of divergences are encountered in QFT, infrared and ultraviolet. UV singularities come from the high energy regime. They may signal that the theory is incomplete at high energies, and can be handled through renormalization. IR divergences in QCD may be soft or collinear. Soft divergences come from the emission of low energy gluons, while collinear divergences arise when a particle emits a gluon in the direction it travels. IR divergences should cancel in sums of diagrams corresponding to well-defined observables.

In a sense, UV divergences are also solved by careful analysis of what is observable. The Lagrangian specifying the theory includes several parameters, such as coupling constants and masses. It is important to realize that these parameters are not physically meaningful. Quantities calculated from the theory with these parameters will often be infinite. Through renormalization, the dependence on unphysical parameters can be eliminated and finite relations between physical values is obtained.

The first step in the renormalization procedure is to regularize the integrals, so that the results can be manipulated algebraically without infinities. This can be done in many ways. The conceptually simplest regularization is to cut the integral off at some value λ. The integrals now converge and observables are calculated as a function of λ and the Lagrangian parameters. Adding the λ-dependence into the parameters, observables are finite functions of the new parameters. The new parameters are finitely related to experimental outcomes and can be measured. The shift in the parameters can also be thought of as adding extra terms in the Lagrangian, called counterterms.

The cut-off λ may be unphysical, or it may represent a true physical cut-off, signaling that the theory is incomplete. Renormalization can be done in either case. Other types of regularization can be chosen, such as the dimensional regularization. The final result does not depend on the specific method.

Dimensional regularization is based on the fact that integrals may be divergent in some dimensions, but convergent in others. In dimensional regularization, the integral is considered as a function of its dimension d. This function can be evaluated for d where it converges and analytically continued to other values. By analytically continuing to $d = 4 - 2\epsilon$, where ϵ is small, the divergence of the original integral is represented by terms like ϵ^{-1}.

An important property of dimensional regularization is the way it handles scaleless integrals. Since the integral should produce an expression of fractional dimension, it must contain dimensional parameters. If it does not, it can be set to zero. A more detailed analysis would show that it in fact contains both UV and IR poles, but that they cancel each other.

This shift in dimension also modifies the dimension of your Lagrangian parameters. Previously dimensionless quantities, like the coupling constant g_0, acquire a fractional dimension. By introducing a new parameter μ, of some appropriate dimension, one can define a dimensionless coupling constant by

$$\frac{\alpha_s}{4\pi} = \frac{\mu^{-2\epsilon} g_0^2}{(4\pi)^{d/2}\Gamma(1+\epsilon)}. \tag{2.3}$$

The factors in the denominator simplify expressions by canceling out several artificial terms. This is called an $\overline{MS}$-scheme.

The independence of the original parameters on μ leads to the renormalization group equation (RGE), a differential equation for how parameters depend on μ. See the next section on the renormalization of Wilson lines for an example. The value of the renormalization group is that it allows one to handle different scales of μ within perturbation theory. The value of μ impacts the convergence properties of the perturbative series. The same series may not be valid for two values of μ that are very different. The RGE solves this problem by only using differential increments of μ.

If the modification of the parameters can be expressed with a renormalization factor, i.e,

$$g_0 = Z_g(\epsilon, g(\mu))g(\mu) \tag{2.4}$$

where g is the renormalized parameter, the theory is multiplicatively renormalizable. We will make use of the renormalization factors for the coupling constant g and the gauge field A_μ. these are well known in QCD to the order we need.

2.1.1 Renormalization of Wilson loops

The renormalization of Wilson loops depends on their path. The case of a smooth non-intersecting loop is the simplest. In dimensional regularization, their renormalization is complete when the coupling constant and the gauge field have been renormalized [1, 12]. The renormalized loop takes the form

$$\Phi_R(C) = \mathcal{P}\exp\left(-iZ_g Z_A^{1/2} g \oint dz^\mu A_\mu(z)\right). \tag{2.5}$$

Wilson loops containing cusps, i.e. points where the contour is not smooth, have additional divergences. A cusp is characterized by its two tangent vectors ν_1 and ν_2. The cusp divergence is a function of the angle γ_{12} between the vectors. This angle is defined in Minkowski space as $\cosh\gamma = \frac{\nu_{12}}{\sqrt{\nu_1^2\nu_2^2}}$, where $\nu_{12} = (\nu_1 \cdot \nu_2)$. If both vectors are off lightcone, the cusp divergence can be multiplicatively renormalized by a factor Z_γ [12]. Loops with a finite amount of cusps off lightcone should be multiplied by the renormalization factor of each cusp.

In the RGE for cusped Wilson lines, the cusp renormalization factors give rise to the cusp anomalous dimension. The RGE comes from the independence of the original loop $\Phi(C) = Z_\gamma\Phi_R(C)$ on μ. Differentiating with respect to μ we have

$$\mu\frac{d}{d\mu}Z_\gamma\Phi_R(\mu^2;C) = \left(\mu\frac{\partial}{\partial\mu} + \beta\frac{\partial}{\partial g} + \Gamma_{\text{cusp}}(\gamma,g)\right)\Phi_R(\mu^2;C) = 0 \tag{2.6}$$

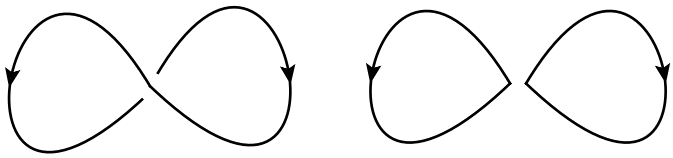

Figure 2: Renormalization of loops with self-intersection mixes all possible ways of connecting incoming with outgoing lines.

where $\Gamma_{\text{cusp}}(\gamma, g) = \frac{\mu}{Z_\gamma}\frac{dZ_\gamma}{d\mu}$ is the cusp anomalous dimension and $\beta = \mu\frac{\partial g}{\partial\mu}$. The cusp anomalous dimension has been known to two-loop order for a long time [14]. To three-loop order it was calculated in [15].

When one or both of the vectors are on lightcone, this equation is not valid anymore. This follows from the fact that as ν approaches lightcone, $\gamma(\nu_1, \nu_2)$ blows up. For large γ, it is proven in [22] that Γ_{cusp} is linear in γ to all orders in perturbation theory. In [14], an explicit calculation shows that Φ_R is finite. The RGE equation can therefore not be satisfied.

Nevertheless, it is possible to find a similar equation that does hold [14]. The trick is to differentiate $\Gamma_{\text{cusp}}(\gamma, g)$ with respect to ν_{12}. This will remove all dependence on ν^2. This removes the problem of $\Gamma_{cusp}(\gamma, g)$ blowing up. Integrate back over ν_{12} to find

$$\left(\mu\frac{\partial}{\partial\mu} + \beta\frac{\partial}{\partial g}\right)\Phi_R(\mu^2; C) = -\Gamma_{cusp}(g)\log\nu_{12} - \Gamma(g) \tag{2.7}$$

where $\Gamma(g)$ is some integration constant. This let's us find $\Gamma_{cusp}(g)$ from knowing Φ_R.

If the Wilson line has endpoints, they will contribute with renormalization factors [11] and a corresponding endpoint anomalous dimension. In this thesis, we study semi-infinite lines with endpoints at infinity. We will introduce a regulator that exponentially suppresses these contributions.

For completeness, we also mention the case where loops self-intersect. This case requires a matrix of renormalization factors [13]. This is because there is mixing between all ways of connecting the incoming lines with outgoing lines, see figure 2.1.1.

2.2 Feynman diagrams

We are looking to calculate the vacuum averages of Wilson lines. Here is where the machinery of QFT comes in. The path integral approach takes us quickly to what we need. As any introductory textbook on QFT explains, the vacuum average of an operator can be calculated as

$$\langle\mathcal{O}\rangle = \frac{1}{Z_0}\int\mathcal{D}A\,\mathcal{O}e^{iS_0[A]+iS_{\text{int}}} \tag{2.8}$$

where Z_0 is the same integral but without the operator $\mathcal{O}$, the integration is over all possible configurations of the fields A, $S_0[A]$ is the free part of the action and $S_{\text{int}}[A]$ is the interaction part of the action. This is very similar to calculating expectation values

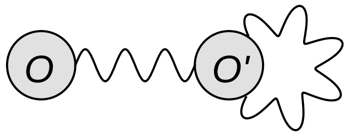

Figure 3: The Feynman graph for $\int \frac{\delta}{\delta A_1}\mathcal{O}[A]\Big|_{A=0} \Delta(x_1,x_2)\Delta(x_3,x_4)\frac{\delta}{\delta A_2}\frac{\delta}{\delta A_3}\frac{\delta}{\delta A_4}\mathcal{O}'[A]\Big|_{A=0}$

in statistical mechanics using the partition function. With functional derivatives we can write as what is called the differential reduction formula [23]

$$\langle T\mathcal{O}[A]\rangle = Z_0^{-1} e^{\int \frac{dxdx'}{2}\frac{\delta}{\delta A_x}\Delta(x,x')\frac{\delta}{\delta A_{x'}}}\mathcal{O}[A]e^{iS_{int}[A]}\Big|_{A=0}. \tag{2.9}$$

A derivation is presented in appendix C. For perturbative calculations, we expand the exponentials in a power series. The functional derivatives satisfy the ordinary product rule for derivatives, generating a large amount of terms. These can be kept track of using Feynman diagrams. When n functional derivatives act on an operator, such as on F or any in S_{int}, denote it by a vertex with n external legs. Each leg inherits the x-coordinate of the corresponding functional derivative. The propagator $\Delta(x,x')$ connects different legs. As an example, with two operators $\mathcal{O}$ and $\mathcal{O}'$, the graph in figure 3 corresponds to the term $\int \frac{\delta}{\delta A_1}\mathcal{O}[A]\Big|_{A=0}\Delta(x_1,x_2)\Delta(x_3,x_4)\frac{\delta}{\delta A_2}\frac{\delta}{\delta A_3}\frac{\delta}{\delta A_4}\mathcal{O}'[A]\Big|_{A=0}$. In the series, each diagrams will enter with some combinatorial prefactor. This factor is related to the symmetries of the diagram and is called the symmetry factor. We do not consider them here, but we will use combinatorial arguments when we discuss exponentiation in section 3.2.

In appendix B we present the Feynman rules for QCD and a derivation of the Feynman rules for the semi-infinite Wilson lines under consideration.

3 Wilson lines

3.1 Definitions, elementary properties

Consider a contour consisting of the points $z(\tau)$ with $\tau \in [0,1]$ and $z(0) = a, z(1) = b$. At each point z on the contour we have the tangent vector $\gamma^\mu(z(\tau))$. Wilson lines satisfy

$$\begin{aligned} \gamma^\mu(z(\tau))\overrightarrow{D}_\mu \Phi(z(\tau), b) &= 0 \\ \Phi(z(\tau), z(\tau)) &= 1 \\ \Phi(a, z(\tau))\Phi(z(\tau), b) &= \Phi(a, b) \end{aligned} \tag{3.1}$$

[24], which we take as a starting point for demonstrating their properties. $D_\mu = \partial_\mu - igA_\mu$ is the covariant derivative. The reason for introducing the parameter τ, rather than just using z, is to avoid ambiguities in the path taken. If the contour loops back on itself, z does not uniquely specify where we came from. The equation $\Phi(z,z) = 1$ only holds when it refers to the trivial path of a single point. Being aware of this, we will drop τ for simplicity.

Based on these equations we derive some basic properties of Wilson lines. The first two equations determine that the covariant derivative acts on the second argument as

$$\gamma^\mu(z)\Phi(a, z)\overleftarrow{D}_\mu = 0 \tag{3.2}$$

The transformation properties of the gauge field A determine the transformation properties of the Wilson line Φ. The gauge field A transforms as

$$A_\mu(z) \to U(z)A_\mu(z)U^\dagger(z) - \frac{i}{g}(\partial_\mu U(z))U^\dagger(z), \tag{3.3}$$

and the covariant derivative as $D_\mu(z) \to U(z)D_\mu(z)U^\dagger(z)$. If the Wilson line transforms as $\Phi \to \Phi'$, the new line satisfies

$$\begin{aligned} \gamma^\mu(z)U\overrightarrow{D}_\mu U^\dagger \Phi'(z, b) &= 0 \\ \gamma^\mu(z)\Phi'(a, z)U\overleftarrow{D^\dagger}_\mu U^\dagger &= 0. \\ \Phi'(a, z)\Phi'(z, b) &= \Phi'(a, b). \end{aligned} \tag{3.4}$$

Clearly, the transformation $\Phi(a, b) \to U(a)\Phi(a, b)U^\dagger(b)$ satisfies all of these equations. Under hermitian conjugate, the first equation in (3.1) becomes

$$\gamma^\mu(z)\Phi^\dagger(z, a)\overleftarrow{D}_\mu = 0. \tag{3.5}$$

Comparing with equation (3.2), we find that

$$\Phi(a, b)^\dagger = \Phi(b, a). \tag{3.6}$$

Wilson lines are unitary, as the following line shows:

$$\Phi(a,b)\Phi(a,b)^\dagger = \Phi(a,b)\Phi(b,a) = \Phi(a,a) = 1. \tag{3.7}$$

From the definition, it is clear that, Φ is invariant under rescaling of the tangent vector.

Knowing the basic properties of Wilson lines, we specialize to the case of semi-infinite straight Wilson lines $\Phi_\nu(0,\infty)$. These are specified by the constant tangent vector ν. The unbounded integration gives rise to a collinear divergence. To regularize it, we introduce a regulator that exponentially suppress the integrand away from the origin. This amounts to including a factor $e^{-\delta\tau}$ for each $A(\tau)$. The regularized Wilson line takes the form

$$\begin{aligned}\Phi_\nu(0,\infty) \;&=\; 1 - ig\int_0^\infty A_\mu e^{-\delta\tau_1} v^\mu d\tau_1 \\ &\qquad - g^2\int_0^\infty d\tau_1 \int_{\tau_1}^\infty d\tau_2 A_\mu(\tau_1)A_\nu(\tau_2)e^{-\delta(\tau_1+\tau_2)}v^\mu v^\nu + \ldots\;.\end{aligned} \tag{3.8}$$

Using the path ordering operator, which orders the fields later along the path to the right of earlier fields, we write the solution compactly as

$$\Phi_\nu(0,\infty) = \mathcal{P}\exp\left(-ig\int_0^\infty A_\mu e^{-\delta\tau} v^\mu d\tau\right). \tag{3.9}$$

The path ordering acts termwise in the expansion of the exponential.

A similar regularization is used in for example [25], but with $\delta\sqrt{\nu^2}$ instead of just δ. This factor is there to make sure the integral is invariant under rescaling of the tangent vector. However, we consider Wilson lines on lightcone where $\nu^2 = 0$. Therefore, this factor is not available to us. Thus, our regularization spoils scale invariance. We will come back to this when we study the cusp with three lines.

3.2 Exponentiation

The exponentiation of disconnected diagrams is standard material in textbooks like [5]. We present similar arguments here, tailored to our purpose. Exponentiating means that a sum of diagrams can be represented as the exponential of another sum of diagrams. Connected diagrams play a crucial role here. If a diagram consists of disconnected pieces, it is equal to the product of those pieces.

Consider an operator of the form $\mathcal{O} = e^{\mathcal{F}}$. For a moment, we assume $\mathcal{F}$ to be a scalar operator, so that there is no trouble with reordering. Expanding $\mathcal{O}$ in a power series, we find terms like $\frac{\mathcal{F}^n}{n!}$. This operator gives rise to diagrams with n insertions of $\mathcal{F}$-vertices. We can factor such a diagram into connected pieces C_i. Denote by k_i the number of $\mathcal{F}$-vertices in the piece and by m_i the number of such pieces in the diagram. Taking into account the combinatorics of how many ways one can partition the $\mathcal{F}$-vertices into the connected pieces, the diagram is

$$\prod_i \frac{C_i^{m_i}}{k_i! m_i!}. \tag{3.10}$$

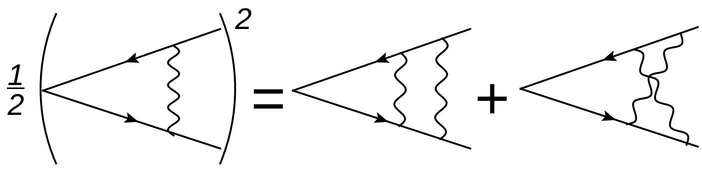

Figure 4: The diagrammatic relation that allows for exponentiation at two-loop order. The crossed diagram should be taken with a modified color factor.

The series for $\langle \mathcal{O} \rangle$ is the sum of all such diagrams. It's easy to see that all terms are generated by

$$\exp\left(\sum_i \frac{C_i}{k!}\right). \tag{3.11}$$

where the sum runs over all connected diagrams. We conclude that operators of the form $\mathcal{O} = e^{\mathcal{F}}$ exponentiate. The original series which includes disconnected diagrams is generated by the exponential of a series of only connected diagrams. Abelian Wilson lines can be exponentiated in this manner [18].

If $\mathcal{F}$ is a matrix, the order of $\mathcal{F}$-vertices is important. Then different partitions of $\mathcal{F}$-vertices are not equivalent. Nonetheless, non-abelian Wilson lines also exponentiate [26, 27, 28], as we will see in the next section.

3.2.1 Non-abelian exponentiation

The non-abelian exponentiation theorem was proven in [27]. That renormalization may be performed in the exponent was shown in [28].The fact that a perturbative series can be presented by the exponential of another series is trivial. One only needs to solve the following equation for w_n.

$$\Phi = 1 + \sum_{n=1}^{\infty} \left(\frac{\alpha_s}{\pi}\right)^n W_n = \exp \sum_{n=1}^{\infty} \left(\frac{\alpha_s}{\pi}\right)^n w_n. \tag{3.12}$$

The non-abelian exponentiation theorem [27] [28] specifies the form of w_n. It states that w_n consists of the same diagrams as W_n, but with modified color factors. The advantage of the approach is that only a subset of diagrams, called webs, have non-zero modified color factors. Webs are those diagrams which cannot be separated into two lower order diagrams by two cuts of Wilson lines. In [28] we also learn that renormalization of the exponent is enough to renormalize the Wilson line.

Considering the cusp anomalous dimension at two-loop order, with the help of webs we can eliminate one diagram. On the diagrammatic level, it works like figure 4 shows. The ladder diagram can be eliminated in the exponent, while the crossed diagram must be taken with a modified color factor.

3.2.2 Generating Function approach

This approach is explained in detail in [18, 19]. Here, we extract only the general idea and some expressions we need.

In the previous section, the Wilson line Φ has been expressed as a path ordered exponent, but it can be represented by an ordinary exponential. The price to pay is that the exponent is more complicated.

$$\Phi(a,b) = \exp\left(\sum_{k=0}^{\infty} \Omega_k(a,b)\right) \tag{3.13}$$

where $\Omega_k \sim g^k$. The series is known as the Magnus series. It resembles the Baker-Campbell-Hausdorff formula, but we don't need the exact form of it. It is important to us that each term consists of completely nested commutators of the gauge field A. Since the generators satisfy

$$\left[t^a, t^b\right] = f^{abc} t^d, \tag{3.14}$$

where f^{abc} is the structure constant (see appendix D for more details), one can extract a single generator out of the nested commutators. Each Ω_k can therefore be written as $\Omega_k = t^a V_k^a$, where $V_k^a \sim g^k$. Only the non-commutativity of the generators prevents the ordinary exponentiation with connected diagrams. The trick is to replace generators by scalars $t^a \to M^a$, one for each generator. We can at any stage go back to matrices by means of the matrix shift operator. The action of the matrix shift operator on a scalar function $f(x)$ is defined by

$$\widetilde{f}(t) = \exp\left(t^a \frac{\partial}{\partial x^a}\right) f(x)\big|_{x=0}, \tag{3.15}$$

where $\widetilde{\ }$ denotes the matrix function. Following [19], we introduce the scalar Wilson line

$$\phi = e^{M^a V_a}. \tag{3.16}$$

Its vacuum expectation value can be exponentiated in the usual manner.

$$\langle \phi \rangle = e^{W[M]} \tag{3.17}$$

where $W[M]$ is a sum over connected diagrams with insertions of V_a-vertices. Shifting back to matrices we have

$$\langle \Phi \rangle = \exp\left(t^a \frac{\partial}{\partial M^a}\right) e^{W[M]}\Big| M = 0 \tag{3.18}$$

The matrix shift and the exponential do not commute, hence $\langle \Phi \rangle \neq \exp\left(\widetilde{W[t]}\right)$. By defining the defect of exponentiation as

$$\widetilde{\delta W}[t] = \left[\log, \exp\left(t^a \frac{\partial}{\partial M^a}\right)\right] e^{W[M]}\Big|_{M=0}, \tag{3.19}$$

we obtain the expectation value of the Wilson line as

$$\langle\Phi\rangle = e^{\widetilde{W[t]}+\widetilde{\delta W}}. \tag{3.20}$$

The defect is a function of $\widetilde{W[t]}$, which is called the kernel of matrix exponentiation (MEK). For perturbative calculations, it is convenient to decompose it into orders of g: $\widetilde{\delta W} = \sum_{n=1}^{\infty} \widetilde{\delta_n W}$, where $\widetilde{\delta_n W} \sim g^n$. A recursive formula for the defect is

$$\widetilde{\delta_n W}[t] = \frac{1}{n!}\{\widetilde{W^n}\} - \sum_{k=2}^{n} \frac{1}{k!} \sum_{\substack{i>1,\\ \sum i=n}} \left(\widetilde{\delta_{i_1} W} ... \widetilde{\delta_{i_k} W}\right), \tag{3.21}$$

where $\widetilde{\delta_1 W} = \widetilde{W}$. We write down the explicit formula at second order as we will use it later,

$$\widetilde{\delta_2 W}[t] = \frac{1}{2}\left(\{\widetilde{W^2}\} - \left(\widetilde{W}\right)^2\right). \tag{3.22}$$

It is useful to represent the MEK in the following form

$$\begin{aligned}
\widetilde{W} \quad = \quad & \sum_{k=1}^{N} t_k^a \langle V_{\gamma_k}^a \rangle + \sum_{\substack{k,l=1\\ k<l}}^{N} t_k^a t_l^b \langle V_{\gamma_k}^a V_{\gamma_l}^b \rangle + \sum_{k}^{N} \frac{(t_k^{\{ab\}}}{2!} \langle V_{\gamma_k}^a V_{\gamma_l}^b \rangle \\
& + \sum_{\substack{k,l,m=1\\ k<l<m}}^{N} t_k^a t_l^b t_m^c \langle V_{\gamma_k}^a V_{\gamma_l}^b V_{\gamma_m}^c \rangle + \sum_{\substack{k,l=1\\ k<l}}^{N} \frac{t_k^{\{ab\}}}{2!} t_l^c \langle V_{\gamma_k}^a V_{\gamma_k}^b V_{\gamma_l}^c \rangle + \sum_{\substack{k,l=1\\ k<l}}^{N} \frac{t_k^a t_l^{\{bc\}}}{2!} \langle V_{\gamma_l}^a V_{\gamma_k}^b V_{\gamma_k}^c \rangle \\
& + \sum_{k=1}^{N} \frac{t_k^{\{abc\}}}{3!} \langle V_{\gamma_k}^a V_{\gamma_k}^b V_{\gamma_k}^c \rangle + ... \, ,
\end{aligned} \tag{3.23}$$

where $t^{\{a_1...a_n\}}$ is the symmetric sum of the generators t^{a_i} weighted by $\frac{1}{n!}$. The dots denote the correlators with higher number of operators V, that are not necessary in this work.

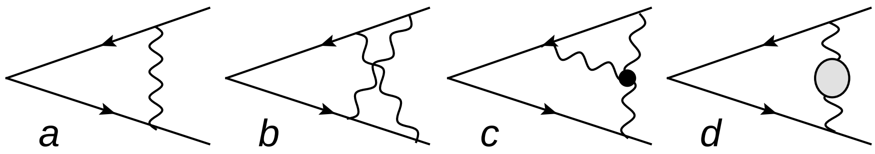

Figure 5: All diagrams contributing to the cusp on lightcone up to two loops. Diagram d is the one-loop contributions to the gluon propagator including counterterms.

4 Cusp for two lines on light cone

In this section we consider a configuration of two lightlike Wilson lines forming a cusp. Their directions will be denoted ν_1 and ν_2. For regulation of ultraviolet divergences we will use dimensional regularization in the $\overline{MS}$-scheme, defined in equation 2.3. Collinear divergences are handled by δ-regularization defined in 3.9. Soft divergences should not appear in our calculation, however to prevent possible problems we used a finite shift of Δ in the Feynman propagator.

We will calculate the cusp on lightcone up to two loops. There are many diagrams which contribute to this quantity. However, for our configuration all diagrams with one or more propagators that start and end at the same Wilson line are zero, since they are proportional to $\nu^2 = 0$. Since we are working in exponentiated form, the ladder diagram is absent and the crossed diagram (b) should be taken with a modified color factor $C_F(C_F - C_A/2) \to -C_F C_A/2$. The constants C_F and C_A are the quadratic Casimirs of the fundamental and adjoint representation respectively D. The remaining non-zero diagrams contributing to the exponent are shown in figure 5.

In the following we present the results of the calculation and comment on the course of evaluation. In appendix A, we present the calculation of diagram c in momentum space.

The same configuration is studied in [29]. The non-lightlike case can be found in [22]. Lightlike polygonal loops are considered in [30] [14] [31] [32].

4.1 One-loop

Only diagram a in figure 5 contributes at the one-loop level. Let us perform the one-loop calculation in coordinate space. The Feynman rules used in the calculation can be found in the appendix B.

The diagram a is the one-gluon-exchange diagram. Its color factor is $t^a_{ik}t^a_{kj} = C_F\delta_{ij}$. Its kinematic part is

$$- g^2\nu_{12}\int dx_{1,2}\int_{\infty}^{0} d\tau_1 \int_0^{\infty} d\tau_2 \delta(\nu_1\tau_1 - x_1)\delta(\nu_2\tau_2 - x_2) D_F(x_1 - x_2) e^{-\delta(\tau_1+\tau_2)} \tag{4.1}$$

where we introduce the shorthand notation $\nu_{12} = \nu_1\nu_2$. The expression for the Feynman propagator in coordinate space reads

$$D_F(x-y) = \frac{\Gamma(1-\epsilon)}{4\pi^{2-\epsilon}} \frac{g^{\mu\nu}\delta_{ab}}{(-(x-y)^2 + i0)^{1-\epsilon}}. \tag{4.2}$$

Integrating expression (4.1) over x we find

$$\frac{-g^2\nu_{12}\Gamma(1-\epsilon)}{4\pi^{2-\epsilon}}\int_0^\infty\int_0^\infty d\tau_1 d\tau_2\frac{e^{-(\tau_1+\tau_2)\delta}}{(2\nu_{12}\tau_1\tau_2+i\Delta)^{1-\epsilon}}=-2g^2\left(\frac{\nu_{12}}{2\delta^2}\right)^\epsilon\frac{\Gamma(1-\epsilon)}{(4\pi)^{2-\epsilon}}\Gamma(\epsilon)^2. \quad (4.3)$$

The Δ regulator can be removed, as the dimension regularization and δ-regularization is enough to regularize the divergences of the integral. Then the evaluation of (4.3) consists of only Γ-function integrals.

From equation (2.7), we find the cusp anomalous dimension at one loop as

$$\Gamma_{cusp}(\alpha)=\frac{\alpha_s}{\pi}C_F. \quad (4.4)$$

This expression coincides with the well known value, see for example [1].

4.2 Two-loop

At two-loop order, we have three diagrams (but note that diagram c also contributes with permuted lines).

The blob in diagram d is the renormalized gluon propagator at one-loop. It adds the contribution of quark-, gluon- and ghost-loops, with corresponding counterterms, within the propagator. In our $\overline{MS}$-scheme the gluon-polarization operator is

$$\Pi^{\mu\nu}_{ab}(k)=i\delta_{ab}\frac{\alpha_s}{4\pi}\left(g^{\mu\nu}k^2-k^\mu k^\nu\right)\left[\left(C_A\left(5-\epsilon\right)-4\left(1-\epsilon\right)T_f n_f\right)\left(\frac{-\mu^2}{k^2+i\Delta}\right)^\epsilon \right.$$
$$\left.\times\frac{\Gamma^2(1-\epsilon)}{\epsilon(3-2\epsilon)\Gamma(1-2\epsilon)}-\frac{1}{\epsilon}\left(\frac{5}{3}C_A-\frac{4}{3}T_F n_f\right)\right] \quad (4.5)$$

where the last term in the parenthesis represents the counterterms. n_f is the number of quark flavors and T_F is the index of the representation D.

In our regularization, the $k^\mu k^\nu$ part of this propagator creates problems. In fact, that term should be removed from the calculation for the following reasons. Recall that δ regulates collinear divergences and Δ regulates soft divergences. The soft divergences cancel in the sum of diagrams while the collinear may remain. With $(k\nu_1)(k\nu_2)$ in the numerator, δ is not needed to regularize the integral. But, we *do* find a δ in the result. We conclude that it has taken over the role of Δ, in regularizing a soft divergence. The soft divergences of this diagram should cancel with those in the $k^\mu k^\nu$ part of the self-interaction diagrams. But since we are one lightcone, those diagrams disappear. We conclude that we must set this part to zero as well, in order to enforce the gauge invariance that was violated by the δ-regularization. In all expressions below, the $k^\mu k^\nu$ contribution has been removed.

The expression for individual diagrams and results of their evaluation are

$$
\begin{aligned}
w_{\text{1-loop}} &= iC_F g^2 \nu_{12} \int \frac{d^d k}{(2\pi)^d} \frac{1}{(k^2+i\Delta)(k\nu_1 - i\delta)(k\nu_2+i\delta)} &(4.6)\\
&= -2\frac{\alpha_s}{4\pi} C_F e^{L\epsilon} \frac{\Gamma(1-\epsilon)\Gamma(\epsilon+1)}{\epsilon^2} &(4.7)\\
w_{\text{cross}} &= \frac{C_F C_A}{2} g^4 \nu_{12}^2 \int \frac{d^d k d^d l}{(2\pi)^{2d}} \frac{1}{(k^2+i\Delta)(l^2+i\Delta)} \\
&\quad \times \frac{1}{(k\nu_1 - i\delta)((k+l)\nu_1 - 2i\delta)(l\nu_2+i\delta)((k+l)\nu_2+2i\delta)} &(4.8)\\
&= -\left(\frac{\alpha_s}{4\pi}\right)^2 \frac{C_A C_F}{2} e^{2L\epsilon} \frac{\Gamma^2(1-\epsilon)\Gamma^2(\epsilon+1)}{\epsilon^4} &(4.9)\\
w_{\text{3g}} &= \frac{C_F C_A}{2} g^4 \nu_{12} \int \frac{d^d k_{1,2,3}}{(2\pi)^{3d}} \frac{\delta(k_1+k_2+k_3)}{(k_1^2+i\Delta)(k_2^2+i\Delta)(k_3^2+i\Delta)} \\
&\quad \times \frac{\nu_1(k_1-k_2)}{(k_1\nu_1 - i\delta)((k_1+k_2)\nu_1 - 2i\delta)(-k_3\nu_2 - i\delta)} &(4.10)\\
&= \left(\frac{\alpha_s}{4\pi}\right)^2 C_A C_F e^{2L\epsilon} \frac{\Gamma(1+2\epsilon)^2\Gamma(1-2\epsilon)}{4\epsilon^3\Gamma^2(1+\epsilon)} \left(\frac{\Gamma(1-\epsilon)\Gamma(1+\epsilon)}{\epsilon}\right. \\
&\quad \left. - \frac{2^{1-2\epsilon}\Gamma^2(1-\epsilon)}{\Gamma(2-2\epsilon)}\right) &(4.11)
\end{aligned}
$$

$$
\begin{aligned}
w_{\text{se}} + w_{\text{se,ct}} &= -C_F g^2 \int \frac{d^d k}{(2\pi)^d} \frac{\nu_1^\mu \nu_2^\nu \Pi_{\mu\nu}(k)}{(k^2+i\Delta)^2(k\nu_1 - i\delta)(k\nu_2+i\delta)} &(4.12)\\
w_{\text{se}} &= -\left(\frac{\alpha_s}{4\pi}\right)^2 C_F e^{2L\epsilon} \frac{\Gamma^2(1-\epsilon)\Gamma^2(1+2\epsilon)}{2\epsilon^3(1-2\epsilon)\Gamma^2(1+\epsilon)} \frac{C_A(5-3\epsilon) - 4n_f T_F(1-\epsilon)}{3-2\epsilon} &(4.13)\\
w_{\text{se,ct}} &= -2\left(\frac{\alpha_s}{4\pi}\right)^2 C_F e^{L\epsilon} \frac{\Gamma(1-\epsilon)\Gamma(1+\epsilon)}{\epsilon^3} \left(\frac{5C_A - 4n_f T_f}{3}\right), &(4.14)
\end{aligned}
$$

where we define for convenience

$$
L = \log\left(\frac{\nu_{12}\mu^2}{2\delta^2}\right).
$$

We observe that the parameter Δ does not appear in our result.

At two-loop level one should also include the the renormalization constants of the gauge field and the gauge coupling. The renormalization factor $Z_g Z_3^{1/2} = 1 - C_A \frac{\alpha_s}{4\pi\epsilon} + \mathcal{O}(\alpha_s^2)$ contributes with a term proportional to the one-loop result. Adding all pieces together we have

$$
\begin{aligned}
\left(\frac{\alpha_s}{4\pi}\right)^2 w_2 &= w_{\text{cross}} + 2w_{\text{3g}} + w_{\text{se}} + w_{\text{se,ct}} + (Z_g^2 Z_3 - 1)w_{1-\text{loop}} &(4.15)\\
&= C_F \left(\frac{\alpha_s}{4\pi}\right)^2 (AL^3 + BL^2 + CL^1) + \text{finite terms.} &(4.16)
\end{aligned}
$$

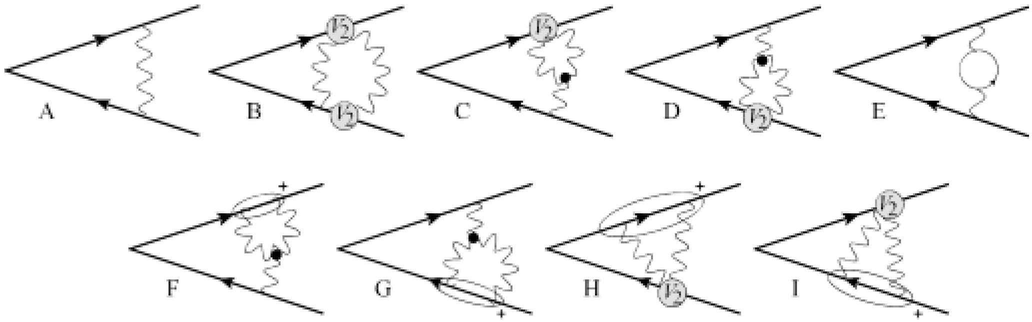

Figure 6: The set of diagrams in the generating function approach. The ellipse means the symmetrized sum of vertex-orderings. Figure taken from [19].

where

$$A = -\frac{(11C_A - 4n_f T_f)}{9}, \qquad B = C_A\left(\frac{2\pi^2}{3} - \frac{67}{9} + \log(4)\right) + \frac{20 n_f T_f}{9},$$
$$C = -\, C_A\left(2\zeta(3) + \frac{11\pi^2}{9} + \frac{404}{27} + 4\log^2(2) - 8\log(2)\right) + n_f T_F\left(112/27 + (4\pi^2)/9\right).$$

The corresponding cusp anomalous dimension is

$$\Gamma_{cusp} = C_F\left(\frac{\alpha_s}{\pi}\right) + \left(\frac{\alpha_s}{\pi}\right)^2 \frac{C_F}{36}(C_A(67 - 6\pi^2 - 36\log(2)) - 20 n_f T_F). \tag{4.17}$$

This expression does not coincide with the well known value of

$$\Gamma_{cusp} = \left(\frac{\alpha_s}{\pi}\right) C_F + \left(\frac{\alpha_s}{\pi}\right)^2 \frac{C_F}{36}(C_A(67 - 3\pi^2) - 20 n_f T_F)$$

first calculated in [14]. One can see that we have an additional term proportional to π^2 and $\log 2$. For the moment, we do not have complete explanation of this discrepancy. However, we suppose that these terms are artificial and arise from the δ-regulator. That observation is novel and have not been discussed in the literature to our best knowledge.

4.2.1 In generating function approach

In the generating function approach, there is a different set of diagrams. These are shown in figure 6. In [19], these diagrams are compared to the previous ones to find how their contributions are encoded in the MEK and the defect. Here we give present short conclusion.

Diagrams F, G, H, I are zero because of the contraction of the anti-symmetric three-gluon vertex with the symmetric sum of generators on one line. Diagrams A,C,D and E are equal to their corresponding diagrams in the ordinary approach.

The main difference of the approach is in the diagram B. This is not surprising, as in the ordinary exponentiation it is the ladder and crossed ladder diagrams that combine to make exponentiation possible. It has been shown in [19] that on lightcone, diagram B is zero. Therefore, the two-gluon exchange diagrams are given entirely by the defect, which is a function of the one-loop result. The defect was calculated in [19] and found to be

$$\widetilde{\delta W_2} = -\frac{C_A}{C_F}\frac{w_1^2}{8}. \tag{4.18}$$

This expression coincides with our expression 4.8. That implies that both approaches to exponentiation are equivalent.

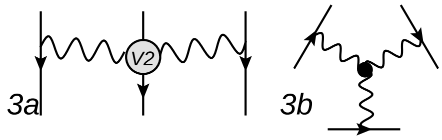

Figure 7: For the three-cusp in the generating function approach, these are the additional diagrams one needs to consider. Both diagrams are zero.

5 Three cusp

We will work entirely in the generating function approach in this case. In the ordinary approach, this case has been studied in [21]. The diagrams contributing to the MEK can be read from equation 3.24. First of all, the diagrams of the previous section should be taken between all pairs of lines. Second, there are three diagrams that connect all three Wilson lines. These are shown in figure 7. We omit the cusp from the diagram, as it is convenient to consider each line in a different matrix space. They can in the end be joined up in the desired order. We will show that the new diagrams either reduce to previously calculated diagrams or vanish.

Diagrams 3a and 3b come from the term $t_1^a t_2^b t_3^c \langle V_{\nu_1}^a V_{\nu_2}^b V_{\nu_3}^c \rangle$, where the subscript on the generators denote which matrix space it's in. These diagrams are the two lowest order contributions from this term from this term. Diagram 3b is considered in appendix A.2.

Diagram 3a is proportional to the integral

$$\int_0^\infty dx_{1,2} dy_{1,2} \frac{(\theta(x_1 > x_2) - \theta(x_2 > x_1)) e^{-\delta(x_1+x_2+y_1+y_2)}}{(2x_1 y_1 \nu_{12} + i0)^{1-\epsilon} (2x_2 y_2 \nu_{23} + i0)^{1-\epsilon}}. \tag{5.19}$$

The $+i0$ can be removed since ϵ regularizes the integral. Removing it, the integral vanishes by symmetry. The same argument is the reason why diagram B vanishes in figure 6. This argument generalizes to all multiple gluon exchange webs [19], i.e. those diagrams with no direct interaction among gluons.

Diagram 3b arises in both the generating function and the ordinary approach. On lightcone, it has been calculated in [21]. They find that it is zero. The details of our calculation is given in appendix 5. Our calculation does not succeed in demonstrating that it vanishes, but numerical tests supports that fact. The stumbling block is related to the δ-regularization. Had we chosen an appropriate δ for each line (e.g. choose $\delta_1 = \delta \left(\frac{\nu_{12}\nu_{13}}{\nu_{23}}\right)^{1/2}$ for line 1), it would vanish by simple symmetry arguments.

We note here a connection to the scale invariance of Wilson lines. As we noted above, the δ-regulator violates this invariance. With factors that scale linearly in ν, such as $\sqrt{\nu^2}$, a regulator that respects scale invariance can be defined. A lightlike Wilson line does not have such a factor. In a configuration of several Wilson lines however, such terms *are* available in the form of $\left(\frac{\nu_{12}\nu_{13}}{\nu_{23}}\right)^{1/2}$. Thus, the same factors that restore scale invariance also greatly simplifies the calculation of diagram 3b. In this case, this violation of scale invariance does not affect the final result, but this may not hold for more complicated diagrams.

We move on to the defect. It is a function of the one-loop expression which we write as

$$w_1 = t_1^a t_2^a w_{12} + t_2^a t_3^a w_{23} + t_1^a t_3^a w_{13} \tag{5.20}$$

where w_{ij} is the one-gluon exchange diagram between lines i and j. For the defect we need w_1^2. It contains two classes of terms, squares and cross terms. We only need to consider one representative from each.

$$w_1^2 = t_1^b t_1^a t_2^a t_2^b w_{12}^2 + (t_1^a t_1^b + t_1^b t_1^a) t_2^a t_3^b w_{12} w_{13} + \dots . \tag{5.21}$$

The squared term contributed to the defect in the previous section, and the expression here is the same:

$$\frac{1}{2}\left(\frac{1}{4}(t_1^a t_1^b + t_1^b t_1^a)(t_2^a t_2^b + t_2^b t_2^a) - t_1^b t_1^a t_2^a t_2^b\right) w_{12}^2 = -\frac{C_A t_1^a t_2^a}{8} w_{12}^2. \tag{5.22}$$

For the cross terms, note that the defect contains only the antisymmetric part of the color factor. The cross term is fully symmetric in color space, hence it cannot contribute to the defect.

Thus, at two-loop order the three-cusp is completely determined by the interactions between pairs of lines. The soft anomalous dimension can be written as

$$\Gamma = \sum_{i \neq j} t_i^a t_j^b \Gamma_{\text{cusp}}(v_{ij}), \tag{5.23}$$

This expression is known as the dipole formula. The violation of the dipole formula is possible at three-loop order. Nowadays, it serves as one of the main tools in the study of multi-hadron processes. This is why any statement about the status of the dipole formula is of great importance.

6 Conclusion

In the thesis, we have presented one- and two-loop calculations involving lightlike Wilson lines. The considered configurations were the cusp, i.e. two Wilson semi-infinite lines merged at origin, and the three-cusp, i.e. three semi-infinite Wilson lines merged at origin. The latter case can be easily generalized on the arbitrary number of Wilson lines. We have considered these configurations both in the traditional approach and in the generating function approach to the exponentiation. We found that these methods agree in the final result, but distribute the contributions differently among diagrams. The generating function approach takes into account the exponentiation structure already at the level of individual diagrams, what makes the analysis simpler.

The two-loop calculation in the generating function approach is done for the first time. As an additional result, our calculation confirms the dipole formula for the soft anomalous dimension [21, 20]. The obtained results will serve as a base for the future publication.

We have considered the problems arising from the use of the δ-regulator. These problems include the violation of gauge invariance and the violation of scale invariance. While for the presented calculation we enforce these manually, we also have discussed possible general solutions to these problems. Summarizing our experience with the δ-regulator, which has been known to be very efficient at one-loop order, we conclude that it may present serious difficulties at higher orders. These difficulties can be solved at two-loop order with reasonable efforts, but in general, they make the use of δ-regulator inconvenient for more involved calculations, such as three-loop calculations or polygons of Wilson loops. We stress that the discussed difficulties arise only for the case of lightlike Wilson lines.

We have observed that the two-loop cusp anomalous dimension calculated within δ-regularization differs from the standard value by terms proportional to π^2 and $\log 2$. Simultaneously, we are fully convinced in the correctness of the presented calculation, since it satisfies all possible checks, and to a high extent can be compared with the similar calculation made by Sterman and Erdoğan [29]. Thus, we conclude that the additional terms are artificial; they are a consequence of the usage of δ-regularization for lightlike Wilson lines. This observation is novel, and puts further doubts on the usage of δ-regulators for lightlike Wilson lines.

The results of the presented work are to be used for the planned calculation of the three-loop soft anomalous dimension. The three-loop soft anomalous dimension is currently unknown, and is one of the most desired object for the high-energy community. The main point is that at three-loop order the soft-anomalous dimension may contain signals of factorization violation [33]. The confirmation of these signals is of utmost importance for the phenomenology of high-energy experiments, such as ALICE or ATLAS at the LHC, where precise predictions of hadronic jets are necessary to interpret experimental data (for a review of recent status see [17]).

Within the generating function approach, the results of the thesis can be used for the calculation of the defect of exponentiation at all-loop order. This is a novel branch of theoretical investigation [19], that may have important applications for low-energy parton dynamics.

A Sample calculations

A.1 $w_{\mathbf{3g}}$ calculation

In this section, we show in detail one way of calculating diagram c in figure 5.

$$I_{3g} = \int \frac{d^d k_{1,2,3}}{(2\pi)^{3d}} \frac{(2\pi)^d \delta(k_1+k_2+k_3)((2k_1\nu_1 - i\delta) - ((k_1+k_2)\nu_1 - 2i\delta))}{(k_1^2+i\Delta)(k_2^2+i\Delta)(k_3^2+i\Delta)(k_1\nu_1 - i\delta)((k_1+k_2)\nu_1 - 2i\delta)(-k_3\nu_2 - i\delta)} \tag{A.1}$$

The integral splits into two simpler ones by cancellation of numerator and denominator. We write it as

$$I_{3g} = 2I_{3g1} - I_{3g2}. \tag{A.2}$$

The calculation is very similar for both integrals, so we will only consider

$$I_{3g1} = \int \frac{d^d k_{1,2,3}}{(2\pi)^{3d}} \frac{(2\pi)^d \delta(k_1+k_2+k_3)}{(k_1^2+i\Delta)(k_2^2+i\Delta)(k_3^2+i\Delta)((k_1+k_2)\nu_1 - 2i\delta)(-k_3\nu_2 - i\delta)}. \tag{A.3}$$

Use α-representation (equation E.1) for each propagator, introducing 5 new integration parameters each with interval $(0,\infty)$. For notational simplicity, we will not explicitly write the corresponding differentials and intervals. In addition, represent the Dirac delta function by $\delta(a) = \int_{-\infty}^{\infty} \frac{d^d x}{(2\pi)^d} e^{-ixa}$. With every momentum in the exponent, complete the squares to get Gaussian integrals over momentum

$$\begin{aligned} I_{3g1} = i^{-1} \int \frac{d^d k_{1,2,3} d^d x}{(2\pi)^{3d}} \exp \Bigg(\\ i\alpha_1 \left(k_1 - \frac{x+\beta_1\nu_1}{2\alpha_1}\right)^2 + i\alpha_2 \left(k_2 - \frac{x+\beta_1\nu_1}{2\alpha_2}\right)^2 + i\alpha_3 \left(k_3 - \frac{x-\beta_2\nu_2}{2\alpha_3}\right)^2 \\ - i\frac{\alpha_{123}}{4\alpha_1\alpha_2\alpha_3} \left(x + \frac{\alpha_1\alpha_2\alpha_3}{\alpha_{123}} \left(\frac{\beta_1\nu_1}{\alpha_1} + \frac{\beta_1\nu_1}{\alpha_2} - \frac{\beta_2\nu_2}{\alpha_3}\right)\right)^2 \\ - i\frac{\alpha_1+\alpha_2}{2\alpha_{123}}\beta_1\beta_2\nu_{12} - \Delta(\alpha_1+\alpha_2+\alpha_3) - \delta(2\beta_1+\beta_2)\Bigg) \end{aligned} \tag{A.4}$$

where $\alpha_{123} = \alpha_1\alpha_2 + \alpha_2\alpha_3 + \alpha_3\alpha_1$. These integrals can be done using equation E.3 giving

$$I_{3g1} = \frac{i^{+d-3}}{(4\pi)^d} \int \alpha_{123}^{-d/2} \exp\Big(- i\frac{\alpha_1+\alpha_2}{2\alpha_{123}}\beta_1\beta_2\nu_{12} - \Delta(\alpha_1+\alpha_2+\alpha_3) - \delta(2\beta_1+\beta_2)\Big). \tag{A.5}$$

Inserting $1 = \int_0^\infty \frac{d\lambda}{\lambda}\delta(1-\lambda\sum\alpha)$ and rescaling $\alpha_n \to \alpha_n/\lambda$ we find

$$I_{3g1} = \frac{i^{d-3}}{(4\pi)^d} \int \lambda^{d-4}\alpha_{123}^{-d/2}\delta(1-\sum\alpha) \exp\Big(-i\lambda\frac{\alpha_1+\alpha_2}{2\alpha_{123}}\beta_1\beta_2\nu_{12} - \Delta/\lambda - \delta(2\beta_1+\beta_2)\Big). \tag{A.6}$$

The regulator Δ is used only for its sign. So we may change $\Delta/\lambda \to \Delta\lambda$. The λ integral followed by the β integrals is straightforward, resulting in

$$I_{3g1} = \frac{2^{2d-7}}{(4\pi)^d}\Gamma(d-3)\Gamma(4-d)^2\delta^{2d-8}\nu_{12}^{3-d} \int \alpha_{123}^{d/2-3}(\alpha_1+\alpha_2)^{3-d}\delta(1-\sum\alpha). \tag{A.7}$$

The Cheng-Wu theorem [34] can be applied here, which states that we may choose any subset of α's in the delta function. It is convenient to choose $\alpha_1 + \alpha_2$. Then the remaining α integrals present no difficulties. The result is

$$\begin{aligned} &\frac{2^{2d-7}}{(4\pi)^d}\Gamma(d-3)\Gamma(4-d)^2\delta^{2d-8}\frac{\nu_{12}^{3-d}}{2-d/2}\frac{\Gamma(d/2-1)^2}{\Gamma(d-2)} \\ &= \nu_{12}^{-1}\frac{2^{1-2\epsilon}}{(4\pi)^{4-2\epsilon}}\Gamma(1-2\epsilon)\Gamma(2\epsilon)^2\left(\frac{\nu_{12}}{2\delta^2}\right)^{2\epsilon}\frac{1}{\epsilon}\frac{\Gamma(1-\epsilon)^2}{\Gamma(2-2\epsilon)}. \end{aligned} \tag{A.8}$$

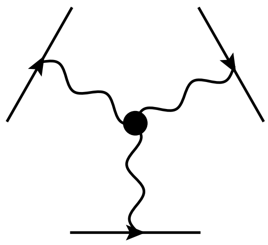

Figure 8: In the configuration of three lightlike Wilson lines with a cusp, this diagram is the most difficult. It cannot be reduced to the exchanges of only two lines. For lightlike lines, it vanishes.

A.2 Three lines connected with a three-gluon vertex

The diagram in figure A.2 is proportional to the expression

$$\nu_1^{\mu_1}\nu_2^{\mu_2}\nu_3^{\mu_3} I_{\mu_1\mu_2\mu_3} \tag{A.9}$$

where

$$I_{\mu_1\mu_2\mu_3} = \int \frac{d^dk_1 d^dk_2 d^dk_3}{(2\pi)^{3d}} \frac{V_{\mu_1\mu_2\mu_3}(-k_1,-k_2,-k_3)(2\pi)^d\delta(k_1+k_2+k_3)}{(k_1^2+i\Delta)(k_2^2+i\Delta)(k_3^2+i\Delta)(k_1\nu_1-i\delta)(k_2\nu_2-i\delta)(k_3\nu_3-i\delta)}. \tag{A.10}$$

The three gluon vertex give rise to terms with the form

$$I_1^\mu = \int \frac{d^dk_1 d^dk_2 d^dk_3}{(2\pi)^{3d}} \frac{k_1^\mu(2\pi)^d\delta(k_1+k_2+k_3)}{(k_1^2+i\Delta)(k_2^2+i\Delta)(k_3^2+i\Delta)(k_1\nu_1-i\delta)(k_2\nu_2-i\delta)(k_3\nu_3-i\delta)}. \tag{A.11}$$

where index 1 on I^μ refers to the which line the k^μ in the numerator is related to. We may decompose this integral into terms proportional to the vectors ν^μ as

$$I_1^\mu = I_{11}\nu_1^\mu + I_{12}\nu_2^\mu + I_{13}\nu_3^\mu. \tag{A.12}$$

Contracting the ν's with the three-vertex shows that the diagram is proportional to

$$\nu_{12}\nu_{23}(I_{12}-I_{32}) + \nu_{23}\nu_{31}(I_{23}-I_{13}) + \nu_{31}\nu_{12}(I_{31}-I_{21}). \tag{A.13}$$

Let's manipulate I_1 into a form where we can extract I_{12}. All I_{ij} with $i \neq j$ can be obtained from it by substitutions. We represent the Dirac delta function by $\delta(k) = \int_{-\infty}^{\infty} \frac{d^dx}{(2\pi)^d} e^{-ixk}$ and use $k_\mu = \frac{\partial}{\partial z^\mu} e^{kz}\big|_{z=0}$ to send all momenta to the exponent. Use α-representation for all propagators, introducing 6 new parameters with integration regions

$(0, \infty)$. Completing the squares in the exponent we get

$$I_{1\mu} = \frac{\partial}{\partial z^\mu} \int \frac{d^d k_{1,2,3} d^d x}{(2\pi)^d} d\alpha_{1,2,3} d\beta_{1,2,3} \exp \Bigg\{ i\alpha_1 \left(k_1 - \frac{x + \beta_1\nu_1 - z}{2\alpha_1} \right)^2 + i\alpha_2 \left(k_2 - \frac{x + \beta_2\nu_2}{2\alpha_2} \right)^2 + i\alpha_3 \left(k_3 - \frac{x + \beta_3\nu_3}{2\alpha_3} \right)^2$$
$$- i\frac{\alpha_{123}}{4\alpha_1\alpha_2\alpha_3} \left(x + \frac{\alpha_1\alpha_2\alpha_3}{\alpha_{123}} \left(-\frac{z}{\alpha_1} + \frac{\beta_1\nu_1}{\alpha_1} + \frac{\beta_2\nu_2}{\alpha_2} + \frac{\beta_3\nu_3}{\alpha_3} \right) \right)^2$$
$$+ i\frac{\alpha_1\alpha_2\alpha_3}{2\alpha_{123}} \left(\frac{\beta_1\beta_2\nu_{12}}{\alpha_1\alpha_2} + \frac{\beta_2\beta_3\nu_{23}}{\alpha_2\alpha_3} + \frac{\beta_3\beta_1\nu_{31}}{\alpha_3\alpha_1} \right) - i\frac{z}{\alpha_1}\frac{\alpha_1\alpha_2\alpha_3}{2\alpha_{123}} \left(-\beta_1\nu_1 \left(\frac{1}{\alpha_2} + \frac{1}{\alpha_3} \right) + \frac{\beta_2\nu_2}{\alpha_2} + \frac{\beta_3\nu_3}{\alpha_3} \right)$$
$$- \Delta\Sigma\alpha - \delta\Sigma\beta \Bigg\} \Bigg|_{z=0} \quad \text{(A.14)}$$

where $\alpha_{123} = \alpha_1\alpha_2 + \alpha_2\alpha_3 + \alpha_3\alpha_1$. Terms with z^2 have been removed as they will vanish when we take the z derivative. With equation E.3 we perform the gaussian integrals to find

$$I_{1\mu} = \frac{i^{d-2}}{(4\pi)^d} \frac{\partial}{\partial z^\mu} \int d\alpha d\beta \alpha_{123}^{-d/2} \exp \Bigg\{ i\frac{\alpha_1\alpha_2\alpha_3}{2\alpha_{123}} \left(\frac{\beta_1\beta_2\nu_{12}}{\alpha_1\alpha_2} + \frac{\beta_2\beta_3\nu_{23}}{\alpha_2\alpha_3} + \frac{\beta_3\beta_1\nu_{31}}{\alpha_3\alpha_1} \right)$$
$$- i\frac{z}{\alpha_1}\frac{\alpha_1\alpha_2\alpha_3}{2\alpha_{123}} \left(-\beta_1\nu_1 \left(\frac{1}{\alpha_2} + \frac{1}{\alpha_3} \right) + \frac{\beta_2\nu_2}{\alpha_2} + \frac{\beta_3\nu_3}{\alpha_3} \right) - \Delta\Sigma\alpha - \delta\Sigma\beta \Bigg\} \Bigg|_{z=0} \quad \text{(A.15)}$$

Taking the z-derivative, we will be able to extract I_{12},

$$I_{1\mu} = \frac{i^{d-3}}{2(4\pi)^d} \int d\alpha d\beta \alpha_{123}^{-d/2-1} \left(-\beta_1\nu_{1\mu} (\alpha_2 + \alpha_3) + \alpha_3\beta_2\nu_{2\mu} + \alpha_2\beta_3\nu_{3\mu} \right)$$
$$\exp \left\{ \frac{i\omega}{2\alpha_{123}} - \Delta\Sigma\alpha - \delta\Sigma\beta \right\}. \quad \text{(A.16)}$$

Where $\omega = \beta_1\beta_2\nu_{12}\alpha_3 + \beta_2\beta_3\nu_{23}\alpha_1 + \beta_3\beta_1\nu_{31}\alpha_2$. From here we read off I_{12} as

$$I_{12} = \frac{i^{d-3}}{2(4\pi)^d} \int d\alpha d\beta \alpha_{123}^{-d/2-1} \alpha_3\beta_2 \exp \left\{ \frac{i\omega}{2\alpha_{123}} - \Delta\Sigma\alpha - \delta\Sigma\beta \right\} \quad \text{(A.17)}$$

Rescale the β's by $\beta_1 \to \sqrt{\frac{\nu_{23}}{\nu_{12}\nu_{13}}}\beta_1$ and similar for the other β's. This removes all scalar products from ω, call the new expression ω'. It is now written as

$$I_{12} = \frac{i^{d-3}}{2(4\pi)^d} \frac{1}{\nu_{12}\nu_{23}} \int d\alpha d\beta \alpha_{123}^{-d/2-1} \alpha_3\beta_2 \exp \Bigg\{ \frac{i\omega'}{2\alpha_{123}} - \Delta\Sigma\alpha$$
$$- \delta \left(\beta_1 \left(\frac{\nu_{23}}{\nu_{12}\nu_{13}} \right)^{1/2} + \beta_2 \left(\frac{\nu_{13}}{\nu_{21}\nu_{23}} \right)^{1/2} + \beta_3 \left(\frac{\nu_{12}}{\nu_{13}\nu_{23}} \right)^{1/2} \right) \Bigg\} \quad \text{(A.18)}$$

We can take this expression and substitute it into A.13 to find that the diagram is proportional to

$$(\nu_{12}\nu_{23}I_{12} - \nu_{23}\nu_{31}I_{13}) \propto \int d\alpha d\beta \alpha_{123}^{-d/2-1}(\alpha_3\beta_2 - \alpha_2\beta_3) \exp\left\{ \frac{i\omega'}{2\alpha_{123}} - \Delta\Sigma\alpha \right. \\ \left. - \delta\left(\beta_1\left(\frac{\nu_{23}}{\nu_{12}\nu_{13}}\right)^{1/2} + \beta_2\left(\frac{\nu_{13}}{\nu_{21}\nu_{23}}\right)^{1/2} + \beta_3\left(\frac{\nu_{12}}{\nu_{13}\nu_{23}}\right)^{1/2}\right)\right\}. \quad \text{(A.19)}$$

This would be antisymmetric (and therefore =0) under the trivial operation of $\alpha_1 \leftrightarrow \alpha_2$, $\beta_1 \leftrightarrow \beta_2$ if it were not for the scalar products in the exponent. This obstacle could be solved by using a different δ for each line or if the scalar products were equal to each other. Then the diagram vanishes by symmetry. Checking numerically, the expression seems to vanish in the form that it is, which is consistent with the conclusions of [21].

B Feynman rules

B.1 QCD

The Feynman rules for QCD is given in any QFT textbook such as [5, 6]. For convenience we reproduce the ones we need here.

Gluon propagator:  $\frac{-i\delta_{ab}}{k^2+i\Delta}g^{\mu\nu}$

This is also called the Feynman propagator and we need it in coordinate space as well:

$$D_{F\,ab}^{\mu\nu}(x-y) = \int_{\infty}^{\infty} \frac{d^d p}{(2\pi)^d} \frac{i}{p^2+i0} e^{-ip(x-y)} = \frac{\Gamma(1-\epsilon)}{4\pi^{2-\epsilon}} \frac{g^{\mu\nu}\delta_{ab}}{(-(x-y)^2+i0)^{1-\epsilon}} \tag{B.1}$$

For two-loop calculations, we need to include the renormalized gluon propagator to one-loop. This term is also called the gluon self-energy. It includes the contributions of all possible loops that can replace the shaded blob. These are gluon, ghost and fermion loops. The number of fermions that contribute is denoted by n_f.

Self-energy: 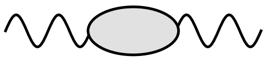 $\Pi_{ab}^{\mu\nu}(k) =$

$$\begin{aligned} = i\delta_{ab}\frac{\alpha_s}{4\pi}\left(g^{\mu\nu}k^2 - k^\mu k^\nu\right)\Bigg[&\left(C_A\left(5-\epsilon\right) - 4\left(1-\epsilon\right)T_f n_f\right)\left(\frac{-\mu^2}{k^2+i\Delta}\right)^{\epsilon} \\ &\times \frac{\Gamma^2(1-\epsilon)}{\epsilon(3-2\epsilon)\Gamma(1-2\epsilon)} - \frac{1}{\epsilon}\left(\frac{5}{3}C_A - \frac{4}{3}T_F n_f\right)\Bigg] \end{aligned} \tag{B.2}$$

Three-gluon vertex:  $V_{\mu_1\mu_2\mu_3}^{a_1a_2a_3}(k_1,k_2,k_3) =$

$$= -gf^{a_1a_2a_3}\left((k_3-k_2)_{\mu_1}g_{\mu_2\mu_3} + (k_1-k_3)_{\mu_2}g_{\mu_3\mu_1} + (k_1-k_3)_{\mu_2}g_{\mu_3\mu_1}\right) \tag{B.3}$$

B.2 Semi-infinite Wilson lines

In this section we present the Feynman rules in both coordinate and momentum space for the lightlike Wilson lines we study. Any number of external gluons may be attached to the line, each case with a different Feynman rule. For n external gluons, the rules for outgoing and incoming Wilson lines are

Outgoing: 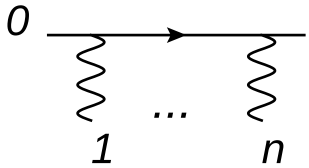

$$\frac{\delta}{\delta A(x_1)} \cdots \frac{\delta}{\delta A(x_n)} \Phi_\nu[0,\infty]\bigg|_{A=0} \theta(x_1 > \cdots > x_n) =$$

$$= (-ig)^n t^{a_n}_{ik_{n-1}} \ldots t^{a_1}_{k_1 j} \nu^{\mu_n} \ldots \nu^{\mu_1} \times \int_0^\infty d\tau_n \ldots \int_{\tau_2}^\infty d\tau_1 \delta(\tau_1\nu - x_1) \ldots \delta(\tau_n \nu - x_n) e^{-\delta \sum_i \tau_i} \tag{B.4}$$

Outgoing Wilson line in momentum space:

$$(-g)^n t^{a_n}_{ik_{n-1}} \ldots t^{a_1}_{k_1 j} \nu^{\mu_n} \ldots \nu^{\mu_1} \frac{1}{p_1\nu - i\delta} \cdots \frac{1}{(p_1 + \cdots + p_n)\nu - in\delta} \tag{B.5}$$

Incoming: 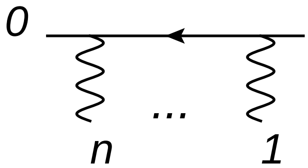

$$\frac{\delta}{\delta A(x_1)} \cdots \frac{\delta}{\delta A(x_n)} \Phi^\dagger_\nu[0,\infty]\bigg|_{A=0} \theta(x_n > \cdots > x_1) =$$

$$(-ig)^n t^{a_1}_{ik_1} \ldots t^{a_n}_{k_{n-1}j} \nu^{\mu_1} \ldots \nu^{\mu_n} \times \int_\infty^0 d\tau_1 \ldots \int_{\tau_{n-1}}^0 d\tau_n \delta(\tau_1\nu - x_1) \ldots \delta(\tau_n\nu - x_n) e^{-\delta \sum_i \tau_i} \tag{B.6}$$

Incoming Wilson line in momentum space:

$$g^n t^{a_1}_{ik_1} \ldots t^{a_n}_{k_{n-1}j} \nu^{\mu_1} \ldots \nu^{\mu_n} \frac{1}{p_1\nu - i\delta} \cdots \frac{1}{(p_1 + \cdots + p_n)\nu - in\delta} \tag{B.7}$$

In the generating function approach, one needs the Feynman rules for the operators V_n. These have more complicated expressions at higher orders. To fourth order, they can be found in [19]. We need only V_1 and V_2, which in coordinate space have the form

$$\begin{aligned} V^{\mu_1}_{a,a_1}(x_1) &= -ig\delta_{aa_1}\nu^{\mu_1}\theta(x1 > 0) \\ V^{\mu_1\mu_2}_{a,a_1a_2}(x_1,x_2) &= -ig^2 f_{aa_1a_2}\nu^{\mu_1}\nu^{\mu_2}(\theta(x_1 > x_2 > 0) - \theta(x_2 > x_1 > 0)) \end{aligned} \tag{B.8}$$

and in momentum space

$$\begin{aligned} V^{a,a_1}_{\mu_1}(p_1) &= \delta^{aa_1}\nu_{\mu_1}\frac{-ig}{(p_1\nu - i\delta)} \\ V^{a,a_1a_2}_{\mu_1\mu_2}(p_1,p_2) &= f^{aa_1a_2}\nu_{\mu_1}\nu_{\mu_2}\frac{ig^2}{(p_1+p_2)\nu - 2i\delta}\left(\frac{1}{p_1\nu_1 - i\delta} - \frac{1}{p_2\nu_1 - i\delta}\right). \end{aligned} \tag{B.9}$$

C Differential reduction formula

We present here a derivation of the differential reduction formula [23], used to calculate vacuum expectation values. In the path-integral formalism, the time ordered expectation value of an operator F is

$$\langle TF[A]\rangle = \frac{1}{Z[0]}\int \mathcal{D}A\, F[A]e^{iS[A]} \tag{C.1}$$

With functional derivatives, we can express $F[A]$ as a shift from $F[0]$,

$$\langle TF[A]\rangle = \frac{1}{Z[0]}\int \mathcal{D}A' e^{iS_0[A']} e^{\int dx A'_x \frac{\delta}{\delta A_x}} F[A]e^{iS_{int}[A]}\bigg|_{A=0} = \left\langle e^{\int dx A'_x \frac{\delta}{\delta A_x}} \right\rangle_0 F[A]e^{iS[A]}\bigg|_{A=0} \tag{C.2}$$

The subscript 0 on the brackets means that the expectation value is taken in the free theory, without interactions. Expanding the exponential in a series, we find terms like

$$\int dx_k ... dx_1 \frac{1}{k!}\left\langle A(x_k)...A(x_1)\right\rangle_0 \frac{\delta}{\delta A_{x_k}} ... \frac{\delta}{\delta A_{x_1}}. \tag{C.3}$$

By Wick's theorem, the correlator is the product of Feynman propagators D_F summed over all pairings of fields. The terms with an odd number of A vanish. The integral over x's makes all pairings identical, replacing the sum over pairings by the number of them, which is $\frac{k!}{2^{k/2}(\frac{k}{2})!}$. Each term then looks like

$$\frac{1}{(\frac{k}{2})!}\left(\int \frac{dxdx'}{2}\frac{\delta}{\delta A_x} D_F(x,x')\frac{\delta}{\delta A_{x'}}\right)^{k/2}. \tag{C.4}$$

This is the expansion of the differential reduction formula

$$\langle TF[A]\rangle = \frac{1}{Z[0]}\, e^{\int \frac{dxdx'}{2}\frac{\delta}{\delta A_x} D_F(x,x')\frac{\delta}{\delta A_{x'}}} F[A]e^{iS_{int}[A]}\bigg|_{A=0}. \tag{C.5}$$

D Algebra

We summarize here some of algebra of the gauge group that we have frequently needed. The algebra is explained in detail in any QFT textbook, see for example. [5, 6]. The generators t^a belong to a representation of the Lie algebra of the SU(n) group. Their commutation relation is

$$[t^a, t^b] = if^{abc}t^c \tag{D.1}$$

where f^{abc} are pure numbers, called the structure constants of the group. f^{abc} antisymmetric under permutation of any two indices.

The sum of the squares of all generators is proportional to the identity matrix

$$t^a_{ik}t^a_{kj} = C_F\delta_{ij}, \tag{D.2}$$

where the coefficient C_F is called the quadratic Casimir of the fundamental representation. The structure constants obey a similar relation

$$f^{abc}f^{abd} = C_A\delta^{cd}, \tag{D.3}$$

where C_A is the quadratic Casimir of the adjoint representation.

The convolution of structure constants and generators is

$$t^a_{ik}t^b_{kj}f^{abc} = i\frac{C_AC_F}{2}t^c_{ij}. \tag{D.4}$$

The index of representation T_F is defined by

$$tr[t^a_r t^b_r] = T_F\delta^{ab}. \tag{D.5}$$

E Useful formulas

This section contains several formulas that have been many times during the course of calculation. An important tool has been the α- or Schwinger representation,

$$\frac{i^{\pm\lambda}}{(A \pm i\Delta)^{\lambda}} = \int_0^{\infty} d\alpha\, \alpha^{\lambda-1} e^{\pm i\alpha A - i\Delta}. \tag{E.1}$$

After the use of α-representation, one encounters Gaussian integrals. In one dimension and in Minkowski space we have

$$\int_{-\infty}^{\infty} dx e^{iax^2} = \sqrt{\frac{\pi}{ia}}, \qquad \mathrm{Im}[a] > 0 \tag{E.2}$$

$$\int_{-\infty}^{\infty} \frac{d^d k}{(2\pi)^d} e^{iak^2} = \frac{1}{(4\pi)^{d/2}} (ia)^{-1/2} (-ia)^{-(d-1)/2} = \frac{i^{d/2-1}}{(4\pi)^{d/2}} a^{-d/2} \tag{E.3}$$

respectively.

Almost all integrals we consider evaluates to products of the Γ function. This is a generalization of the factorial function to the complex plane. As such, it satisfies

$$\Gamma(z+1) = z\Gamma(z). \tag{E.4}$$

We will often encounter the integral representation

$$\Gamma(z) = \int_0^{\infty} t^{z-1} e^{-t} dt. \tag{E.5}$$

For small values of z, it may be expanded in a Laurent series as

$$\Gamma(z) = \frac{1}{z} - \gamma z + \frac{1}{2}(\gamma^2 + \frac{\pi^2}{6}) z^2 + \dots \tag{E.6}$$

$$\ln \Gamma(1+z) = -\gamma z + \sum_{k=2}^{\infty} \frac{\zeta(k)}{k} (-z)^k + \dots \tag{E.7}$$

A related function is the Euler B-function. It can be written as a product of Γ-functions and has a useful integral representation

$$B(a,b) = \int_0^1 x^{a-1} (1-x)^{b-1} dx = \frac{\Gamma(a)\Gamma(b)}{\Gamma(a+b)}. \tag{E.8}$$

References

[1] A. M. Polyakov, “Gauge fields as rings of glue,” *Nuclear Physics B* **164** (1980) 171–188. 3, 4, 7, 16

[2] J. Collins, “Foundations of perturbative QCD,”. 3

[3] J. C. Collins, D. E. Soper, and G. Sterman, “Factorization of Hard Processes in QCD,” *arXiv:hep-ph/0409313* (Sept., 2004) . arXiv: hep-ph/0409313. 3

[4] J. C. Collins, D. E. Soper, and G. F. Sterman, “Transverse Momentum Distribution in Drell-Yan Pair and W and Z Boson Production,” *Nucl.Phys.* **B250** (1985) 199. 3

[5] M. E. Peskin and D. V. Schroeder, *An Introduction To Quantum Field Theory.* Westview Press, Reading, Mass, first edition edition ed., Oct., 1995. 3, 6, 11, 28, 31

[6] M. D. Schwartz, *Quantum Field Theory and the Standard Model.* Cambridge University Press, New York, 1 edition ed., Dec., 2013. 3, 6, 28, 31

[7] S. Mandelstam, “Quantum electrodynamics without potentials,” *Annals of Physics* **19** no. 1, (July, 1962) 1–24. 3

[8] Y. M. Makeenko and A. A. Migdal, “Quantum chromodynamics as dynamics of loops,” *Nuclear Physics B* **188** no. 2, (Sept., 1981) 269–316. 3

[9] R. A. Brandt, A. Gocksch, M. A. Sato, and F. Neri, “Loop space,” *Physical Review D* **26** no. 12, (Dec., 1982) 3611–3640. 3

[10] K. G. Wilson, “Confinement of quarks,” *Physical Review D* **10** no. 8, (Oct., 1974) 2445–2459. 4

[11] G. P. Korchemsky and A. V. Radyushkin, “Loop-space formalism and renormalization group for the infrared asymptotics of QCD,” *Physics Letters B* **171** no. 4, (May, 1986) 459–467. 4, 8

[12] V. S. Dotsenko and S. N. Vergeles, “Renormalizability of phase factors in non-abelian gauge theory,” *Nuclear Physics B* **169** no. 5–6, (Aug., 1980) 527–546. 4, 7

[13] R. A. Brandt, F. Neri, and M.-a. Sato, “Renormalization of Loop Functions for All Loops,” *Phys.Rev.* **D24** (1981) 879. 4, 8

[14] I. A. Korchemskaya and G. P. Korchemsky, “On light-like Wilson loops,” *Physics Letters B* **287** no. 1–3, (Aug., 1992) 169–175. 4, 8, 15, 18

[15] A. Grozin, J. M. Henn, G. P. Korchemsky, and P. Marquard, “The three-loop cusp anomalous dimension in QCD,” *Physical Review Letters* **114** no. 6, (Feb., 2015) . arXiv: 1409.0023. 4, 8

[16] E. Gardi, “Progress on soft gluon exponentiation and long-distance singularities,” *arXiv:1401.0139 [hep-ph, physics:hep-th]* (Dec., 2013) . arXiv: 1401.0139. 4

[17] L. Magnea, “Progress on the infrared structure of multi-particle gauge theory amplitudes,” *arXiv:1408.0682 [hep-ph]* (Aug., 2014) . arXiv: 1408.0682. 4, 22

[18] A. A. Vladimirov, “Generating function for web diagrams,” *Physical Review D* **90** no. 6, (Sept., 2014) . arXiv: 1406.6253. 4, 5, 12, 13

[19] A. A. Vladimirov, “Exponentiation for products of Wilson lines within the generating function approach,” *arXiv:1501.03316 [hep-ph, physics:hep-th]* (Jan., 2015) . arXiv: 1501.03316. 4, 5, 13, 18, 19, 20, 22, 29

[20] T. Becher and M. Neubert, “Infrared singularities of scattering amplitudes in perturbative QCD,” *Physical Review Letters* **102** no. 16, (Apr., 2009) . arXiv: 0901.0722. 4, 22

[21] S. M. Aybat, L. J. Dixon, and G. Sterman, “The Two-loop Anomalous Dimension Matrix for Soft Gluon Exchange,” *Physical Review Letters* **97** no. 7, (Aug., 2006) . arXiv: hep-ph/0606254. 4, 20, 22, 27

[22] G. P. Korchemsky and A. V. Radyushkin, “Renormalization of the Wilson loops beyond the leading order,” *Nuclear Physics B* **283** (1987) 342–364. 8, 15

[23] A. N. Vasil'ev, *The Field Theoretic Renormalization Group in Critical Behavior Theory and Stochastic Dynamics.* Chapman and Hall/CRC, Waltham, MA, 1 edition ed., Apr., 2004. 9, 30

[24] T. Becher, A. Broggio, and A. Ferroglia, *Introduction to Soft-Collinear Effective Theory.* Springer, 2015 edition ed., Mar., 2015. 10

[25] E. Gardi, J. M. Smillie, and C. D. White, “On the renormalization of multiparton webs,” *arXiv:1108.1357 [hep-ph, physics:hep-th]* (Aug., 2011) . arXiv: 1108.1357. 11

[26] G. F. Sterman, “Infrared Divergences in Perturbative {QCD}. (Talk),” *AIP Conf.Proc.* **74** (1981) 22–40. 12

[27] J. G. M. Gatheral, “Exponentiation of eikonal cross sections in nonabelian gauge theories,” *Physics Letters B* **133** no. 1–2, (Dec., 1983) 90–94. 12

[28] J. Frenkel and J. C. Taylor, “Non-abelian eikonal exponentiation,” *Nuclear Physics B* **246** no. 2, (Nov., 1984) 231–245. 12

[29] O. Erdoğan and G. Sterman, “Gauge theory webs and surfaces,” *Physical Review D* **91** no. 1, (Jan., 2015) . arXiv: 1112.4564. 15, 22

[30] A. Andraši and J. C. Taylor, “Difficulties of renormalization of light-like Wilson loops,” *Nuclear Physics B* **350** no. 1–2, (Feb., 1991) 73–81. 15

[31] A. Bassetto, I. A. Korchemskaya, G. P. Korchemsky, and G. Nardelli, "Gauge invariance and anomalous dimensions of a light-cone Wilson loop in light-like axial gauge," *Nuclear Physics B* **408** no. 1, (Nov., 1993) 62–90. 15

[32] A. Andraši and J. C. Taylor, "Renormalization of Wilson operators in minkowski space," *Nuclear Physics B* **516** no. 1–2, (Apr., 1998) 417–425. 15

[33] L. J. Dixon, E. Gardi, and L. Magnea, "On soft singularities at three loops and beyond," *JHEP* **1002** (2010) 081. 22

[34] V. A. Smirnov, "Evaluating multiloop Feynman integrals by Mellin-Barnes representation," *arXiv:hep-ph/0406052* (June, 2004) . arXiv: hep-ph/0406052. 24